ECOLE POLYTECHNIQUE
PROMOTION 2006
AUGER Violaine

Rapport de stage de recherche

Shear-driven long-lived turbulence from magnetic buoyancy

NON-CONFIDENTIEL

Option : Physique
Champ de l'option : Astrophysique
Directeur de l'option : Caroline Terquem
Directeur de stage : Axel Brandenburg
Dates du stage : 28 mai - 13 juin 2009
Adresse de l'organisme
Nordita
Albanova University centre
106 91 Stockholm
Sweden

Résumé

Le Soleil présente un fort champ magnétique, mais son origine n'est pas encore complètement comprise. Certains scientifiques sont donc amenés à penser qu'il manque certains phénomènes physiques dans les divers modèles proposés. Basé sur un article de 2003, écrit par Cline, Brummel et Cattaneo, nous avons essayé de comprendre l'influence que pouvait avoir le cisaillement dans les phénomènes de base qui peuvent avoir une influence dans la dynamo solaire. A l'aide de simulations avec le Pencil Code, il nous a été possible de voir un puissant champ magnétique se développer en présence de cisaillement et d'un champ poloïdal initial. Ce rapport présente certains phénomènes physiques qui peuvent expliquer cette évolution à long terme du champ magnétique, et décrit ce qui semble se passer.

Summary

The Sun possesses a strong magnetic field, but its origin is not yet fully understood. This leds some scientists to believe that some physics is still missing in the various models that have been proposed. Based on an article of 2003, written by Cline, Brummell and Cattaneo, we tried to understand the influence of the shear on basic processes in the solar dynamo. Thanks to simulations with the Pencil Code, we were able to see a strong magnetic field increase in presence of shear and of an initial poloidal field. This report presents some of the physics which can explain this long-lived magnetic field, and describes what seems to happen.

I want to thank Axel Brandenburg for having supervised me during this internship. I really appreciate all time he took to explain to me all the physics and informatics I needed to make this project.

I also want to thank Caroline Terquem for having found this internship for me.

Finally, I want to thank Boris Dintrans who explained me everything in french about the Pencil Code during a meeting in Finland.

Contents

Introduction

1 Theory

1.1 Magnetic equations

In this paragraph we are going to present the induction equation. The induction equation binds the evolution of $\boldsymbol{B}$ with other magnetohydrodynamic variables. To obtain it, we need three equations :

- Faraday's equation, which describes how the temporal evolution of the magnetic field is linked to the spatial evolution of the electric field.
$$\frac{\partial \boldsymbol{B}}{\partial t} = -\boldsymbol{\nabla} \times \boldsymbol{E} \tag{1}$$
- Ampere's law, describes the spatial evolution of the magnetic field. Due to the factor $1/c^2$, and to the fact that in a conductive material, $\boldsymbol{J}$ and $\boldsymbol{E}$ are proportional, we will always neglect the Ampere's current in this equation.
$$\boldsymbol{\nabla} \times \boldsymbol{B} = \mu_0 \boldsymbol{J} + \frac{1}{c^2}\frac{\partial \boldsymbol{E}}{\partial t} \approx \mu_0 \boldsymbol{J} \tag{2}$$
- Ohm's law, in a conductive material. We will also assume that the conductivity σ is constant in the material.
$$\boldsymbol{E} = \frac{1}{\sigma}\boldsymbol{J} - \boldsymbol{u} \times \boldsymbol{B} \tag{3}$$

Combining these three equations, and with the fact that $\boldsymbol{\nabla} \cdot \boldsymbol{B} = 0$, we now obtain

$$\frac{\partial \boldsymbol{B}}{\partial t} = \boldsymbol{\nabla} \times (\boldsymbol{u} \times \boldsymbol{B}) + \frac{1}{\mu_0 \sigma}\boldsymbol{\nabla} \times (\boldsymbol{\nabla} \times \boldsymbol{B}) \tag{4}$$

and by defining $\eta = \frac{1}{\mu_0 \sigma}$, this leads us to the induction equation.

$$\frac{\partial \boldsymbol{B}}{\partial t} = \boldsymbol{\nabla} \times (\boldsymbol{u} \times \boldsymbol{B}) + \eta \boldsymbol{\nabla}^2 \boldsymbol{B} \tag{5}$$

1.2 Fluid Magnetohydrodynamics

In Magnetohydrodynamics, we also use the classical hydrodynamic equations. First of all, mass conservation implies

$$\frac{\partial \rho}{\partial t} + \boldsymbol{u} \cdot \boldsymbol{\nabla} \rho = -\rho \boldsymbol{\nabla}.\boldsymbol{u} \tag{6}$$

Then there is the impulsion conservation, in which we take all the forces into account : the gravity, which will be in the following considered as constant, the magnetic force, the pressure force and the dissipative term :

$$\frac{\partial \boldsymbol{u}}{\partial t} + \boldsymbol{u} \cdot \boldsymbol{\nabla} \boldsymbol{u} = -\frac{1}{\rho} \boldsymbol{\nabla} P + \boldsymbol{g} + \frac{1}{\rho} \boldsymbol{J} \times \boldsymbol{B} + \nu (\boldsymbol{\nabla}^2 \boldsymbol{u} + \frac{1}{3} \boldsymbol{\nabla} \cdot \boldsymbol{\nabla} \cdot \boldsymbol{u} + \overleftrightarrow{S} \boldsymbol{\nabla} ln \rho \nu) \tag{7}$$

At last, there is the entropy conservation, which will be preferred to the temperature equation, because it was easier to implement it with the Code :

$$\frac{\partial s}{\partial t} + \boldsymbol{u} \cdot \boldsymbol{\nabla} s = 0 \tag{8}$$

1.3 Dimensionless numbers

To have an idea of the behaviour of the magnetic fluid, a set of dimensionless numbers are useful :

1.3.1 Reynolds number

Reynolds number is defined as the ratio of inertial momentum to diffusivity.

$$Re = \frac{UL}{\nu} \tag{9}$$

where U is a characteristic speed of the fluid, L a characteristic length scale, and ν the diffusivity of the fluid.

1.3.2 Magnetic Reynolds number

$$Re_m = \frac{convection}{diffusion} = \frac{\tau_{diff}}{\tau_{conv}} \tag{10}$$

$$Re_m = \mu_0 \sigma U L \tag{11}$$

where σ is the plasma conductivity, U a characteristic speed, and L the depth of the nap.

1.3.3 Prandtl number

$$Pr = \frac{viscous\ diffusion\ rate}{thermal\ diffusion\ rate} \tag{12}$$

$$Pr = \frac{\nu}{\alpha} = \frac{c_P\ \mu}{k} \tag{13}$$

where ν is the kinematic viscosity, k the thermal conductivity, and α the thermal diffusivity.

1.3.4 Magnetic Prandtl number

The magnetic Prandtl number estimates the ratio of momentum diffusivity to magnetic diffusivity.

$$Pr_m = \frac{momentum\ diffusivity}{magnetic\ diffusivity} = \frac{\nu}{\eta} = \frac{Re_m}{Re} \tag{14}$$

with $\eta = \frac{1}{\mu_0 \sigma}$

1.3.5 Chandrasekhar number

$$Q = \frac{Lorentz force}{viscosity} \tag{15}$$

$$Q = \frac{B^2 d^2}{\mu_0 \rho \nu \eta} = \frac{B_0^2 d^2}{\mu_0 \mu \eta} \tag{16}$$

where η is the magnetic diffusivity, ν the kinematic viscosity

1.3.6 Rayleigh number

$$Ra = \frac{buoyancy force}{thermal * momentum\ diffusivity} \tag{17}$$

The buoyancy force is due to the difference of density, or of temperature, and can be expressed either like $g\Delta\rho V$ or like $gV\rho_0\beta\Delta T$, with β the thermal expansion coefficient. The thermal diffusivity is k, and the momentum diffusivity is ν.

We can now write the Rayleigh number :

$$Ra = \frac{\rho_0 g \beta \Delta T D^3}{\nu k} \tag{18}$$

where D the depth of the material.

1.3.7 Peclet number

$$Pe = Re \times Pr = \frac{LV}{\alpha} \tag{19}$$

$$\alpha = \frac{k}{\rho\ c_P}$$

where k is the thermal conductivity, ρ the density and c_P the heat capacity.

1.4 the ω-effect

Observations have shown that the sun cannot be considered as a solid in rotation. On the contrary, there is a differential rotation, which is meaningful. The equator rotates quicker, and then there is a differential rotation until the poles. Therefore, there is a shear in the velocity field, which is localised in the tachocline. The purpose of our simulations is to understand the consequences of this effect on the solar dynamo.

To understand this, we will work with a linear velocity shear, and try to predict the effects on the magnetic field.

For instance, we can use a magnetic field

$$\boldsymbol{B} = \begin{pmatrix} B_x \\ B_y \\ B_z \end{pmatrix}$$

and a velocity field

$$\boldsymbol{U} = \begin{pmatrix} U_x = 0 \\ U_y = S \times x \\ U_z = 0 \end{pmatrix}$$

Then the equations will give us

$$\boldsymbol{U} \times \boldsymbol{B} = \begin{pmatrix} 0 \\ Sx \\ 0 \end{pmatrix} \times \begin{pmatrix} B_x \\ B_y \\ B_z \end{pmatrix} = \begin{pmatrix} S\ x\ B_z \\ 0 \\ -S\ x\ B_x \end{pmatrix} \tag{20}$$

To simplify, let's assume that $B_z = 0$.. It will then ensue that

$$\boldsymbol{\nabla} \times (\boldsymbol{U} \times \boldsymbol{B}) = \begin{pmatrix} \frac{\partial}{\partial x} \\ \frac{\partial}{\partial y} \\ \frac{\partial}{\partial z} \end{pmatrix} \times \begin{pmatrix} S\ x\ B_z \\ 0 \\ -S\ x\ B_x \end{pmatrix} = \begin{pmatrix} -\frac{\partial}{\partial y}(S\ x\ B_x) \\ \frac{\partial}{\partial x}(S\ x\ B_x) \\ 0 \end{pmatrix} \tag{21}$$

So we now see that such a shear changes the magnetic field, and modifies it with the predominant term $S\ Bx$. The magnetic field will behave according to the shear field.

This ω-effect can just create a field orthogonal to the direction of the shear. For instance with the sun, the direction of the shear is radial. It means that the created field will be toroidal. But it won't create a poloidal field. Considering only the ω-effect does not allow to explain the solar dynamo.

1.5 The α-effect

Now let's analyse what happens when $\boldsymbol{U}(\boldsymbol{x},t)$ and $\boldsymbol{B}(\boldsymbol{x},t)$ are turbulent. We can then part these fields, and write them as

$$\boldsymbol{B}(\boldsymbol{x},t) = \overline{\boldsymbol{B}}(\boldsymbol{x},t) + \boldsymbol{b}(\boldsymbol{x},t) \tag{22}$$

$$\boldsymbol{U}(\boldsymbol{x},t) = \overline{\boldsymbol{U}}(\boldsymbol{x},t) + \boldsymbol{u}(\boldsymbol{x},t) \tag{23}$$

using the induction equation,

$$\frac{\partial \boldsymbol{B}}{\partial t} = \boldsymbol{\nabla} \times (\boldsymbol{U} \times \boldsymbol{B}) + \eta \boldsymbol{\nabla}^2 \boldsymbol{B} \tag{24}$$

and take its mean and fluctuating parts. We have then the mean equation

$$\frac{\partial \overline{\boldsymbol{B}}}{\partial t} = \boldsymbol{\nabla} \times (\overline{\boldsymbol{U}} \times \overline{\boldsymbol{B}}) + \boldsymbol{\nabla} \times \overline{\mathcal{E}} + \eta \boldsymbol{\nabla}^2 \overline{\boldsymbol{B}} \tag{25}$$

with

$$\overline{\mathcal{E}} = \langle \boldsymbol{u} \times \boldsymbol{b} \rangle$$

and the fluctuating equation

$$\frac{\partial \boldsymbol{b}}{\partial t} = \boldsymbol{\nabla} \times (\overline{\boldsymbol{U}} \times \boldsymbol{b}) + \boldsymbol{\nabla} \times (\boldsymbol{u} \times \overline{\boldsymbol{B}}) + \boldsymbol{\nabla} \times \boldsymbol{G} + \eta \boldsymbol{\nabla}^2 \boldsymbol{b} \tag{26}$$

with

$$\boldsymbol{G} = \boldsymbol{u} \times \boldsymbol{b} - \langle \boldsymbol{u} \times \boldsymbol{b} \rangle$$

What is really interesting, is that we can now see that one source of the dynamo comes from the turbulence, with the coupled term $\overline{\mathcal{E}} = \langle \boldsymbol{u} \times \boldsymbol{b} \rangle$. It is the mean electromotive force. If we can express this term with the mean values $\overline{\boldsymbol{U}}$ and $\overline{\boldsymbol{B}}$, then we would be able to integrate this equation, and to know the temporal evolution of $\overline{\boldsymbol{B}}$.

The electromotive force can be written as :

$$\epsilon_i = \alpha_{ij} \overline{B}_j + \beta_{ijk} \frac{\partial \overline{B}_j}{\partial x_k} + ... \tag{27}$$

where these coefficients are pseudo-tensors. They can be determined from the mean field $\overline{\mathbf{U}}$, the statistical properties of $\boldsymbol{u}$ and η.

If we now consider the leading term, which is

$$\epsilon_i^{(0)} = \alpha_{ij} \overline{B}_j$$

we can develop it into symmetric and antisymmetric parts, and write consequently

$$\epsilon_i^{(0)} = \alpha_{ij}^s \overline{B}_j + (\boldsymbol{a} \times \overline{\boldsymbol{B}})_i \tag{28}$$

We can then define an effective mean velocity, $\overline{\boldsymbol{U}}_{\text{eff}} = \overline{\boldsymbol{U}} + \boldsymbol{a}$, and we just have one term left.

We have already seen that for one-dimensional averages we can write the electromotive force as a function of the mean of the magnetic field:

$$\overline{\epsilon_i} = \alpha_{ij} \overline{B_j} - \eta_{ij} \overline{J_j} \tag{29}$$

The simulations we did are anisotropic because of the gravity, which is in the z-direction. As a consequence, all the averages were calculated by averaging over all x and y. $\overline{B}$ is no longer a function of x and y. We have now:

$$\boldsymbol{\nabla} \times \overline{\boldsymbol{B}} = \begin{pmatrix} -\partial \overline{B_y}/\partial z \\ \partial \overline{B_x}/\partial z \\ 0 \end{pmatrix} \tag{30}$$

With Faraday's law, $\boldsymbol{\nabla} \times \overline{\boldsymbol{B}} = \mu_0 \overline{\boldsymbol{J}}$, it leads to this new form :

$$\overline{\epsilon_i} = \alpha_{ij} \overline{B_j} - \eta_{ij} \overline{J_j} \tag{31}$$

if we put the factor μ_0 inside the vector $\overline{\boldsymbol{J}}$. The new coefficients η_{ij} are related to the old ones by $\eta_{i1} = \eta_{i23}$ and $\eta_{i2} = -\eta_{i13}$.

1.6 Magnetic helicity

In this paragraph, we study the magnetic helicity, and its properties.

As in the hydrodynamic equations, where we can define the helicity

$$I_m = \int_{V_m} \boldsymbol{u}.\boldsymbol{\omega} \; d\tau$$

where $\boldsymbol{\omega} = \boldsymbol{\nabla} \times \boldsymbol{u}$, we will define the magnetic helicity as :

$$I_m = \int_{V_m} \boldsymbol{A}.\boldsymbol{B} \; d\tau \tag{32}$$

where V_m is a characteristic volume. This magnetic helicity will have a large value if the lines of the magnetic field are twisted and shrunk. It can be positive or negative, depending on the handedness of the magnetic lines.

In the general magnetohydrodynamic case, following equations govern the evolution of the magnetic field :

- the equation of the conducting material, which obeys to Ohm's law :
$$\boldsymbol{J} = \sigma(\boldsymbol{E} + \boldsymbol{u}) \times \boldsymbol{B}) \tag{33}$$
- Poisson's law, which comes from Ampere's law
$$\boldsymbol{\nabla}^2 \boldsymbol{A} = -\mu_0 \boldsymbol{J} \tag{34}$$
- the equation of the electric field, which comes from Faraday's equation
$$\boldsymbol{E} = -\boldsymbol{\nabla}\Phi - \frac{\partial \boldsymbol{A}}{\partial t} \tag{35}$$

With these three equations, we can now find a law for the evolution of the potential vector $\boldsymbol{A}$, which is written without any approximation. Everything comes from Maxwell equations and Ohm's law.

$$\frac{\partial \boldsymbol{A}}{\partial t} = \boldsymbol{u} \times (\boldsymbol{\nabla} \times \boldsymbol{A}) - \boldsymbol{\nabla}\Phi + \lambda \boldsymbol{\nabla}^2 \boldsymbol{A} \tag{36}$$

$$\lambda = \frac{1}{\mu_0 \sigma} \tag{37}$$

In the case of high conductivity, we can consider $\lambda = 0$. This approximation means that we neglect the dissipation term. It will be a valid approximation if

$$\frac{\boldsymbol{u} \times (\boldsymbol{\nabla} \times \boldsymbol{A})}{\lambda \boldsymbol{\nabla}^2 \boldsymbol{A}} << 1$$

To have an idea of the value of this ratio, we can estimate it roughly by

$$\frac{\boldsymbol{u} \times (\boldsymbol{\nabla} \times \boldsymbol{A})}{\lambda \boldsymbol{\nabla}^2 \boldsymbol{A}} \approx \frac{u_0 l_0}{\lambda} = u_0 l_0 \mu_0 \sigma = R_m \tag{38}$$

with R_m the magnetic Reynolds number. If R_m is higher than 1, then our approximation is valid, and the following calculations are right. Otherwise, the dissipation is too high to be neglected.

With this simplification, we can now calculate the material derivatives of $\boldsymbol{A}$ and $\boldsymbol{B}$.

$$\frac{D\boldsymbol{A}}{Dt} = \frac{\partial \boldsymbol{A}}{\partial t} + (\boldsymbol{u} \cdot \boldsymbol{\nabla})\boldsymbol{A} = -\boldsymbol{\nabla}\Phi + \boldsymbol{u} \cdot (\boldsymbol{\nabla} \boldsymbol{A}) \tag{39}$$

$$\frac{D\boldsymbol{B}}{Dt} = \frac{\partial \boldsymbol{B}}{\partial t} + (\boldsymbol{u}\cdot\boldsymbol{\nabla})\boldsymbol{B} = -\boldsymbol{\nabla}\times\boldsymbol{E} + (\boldsymbol{u}\cdot\boldsymbol{\nabla})\boldsymbol{B} = (\boldsymbol{B}\cdot\boldsymbol{\nabla})\boldsymbol{u} - \boldsymbol{B}(\boldsymbol{\nabla}\cdot\boldsymbol{u}) \tag{40}$$

We will also need to know the evolution of the density. The mass conservation gives us the well-known equation :

$$\frac{\partial \rho}{\partial t} + \boldsymbol{\nabla}\cdot(\rho\boldsymbol{u}) = 0 = \frac{\partial \rho}{\partial t} + \rho\boldsymbol{\nabla}\cdot\boldsymbol{u} + \boldsymbol{u}\cdot\boldsymbol{\nabla}\rho \tag{41}$$

and we can deduce from it the material derivative :

$$\frac{D\rho}{Dt} = \frac{\partial \rho}{\partial t} + \boldsymbol{u}\cdot\boldsymbol{\nabla}\rho = -\rho\boldsymbol{\nabla}\cdot\boldsymbol{u} \tag{42}$$

We are now able to calculate all the derivatives we will need to calculate the variation of the magnetic helicity in a volume.

$$\frac{D}{Dt}(\frac{\boldsymbol{B}}{\rho}) = \frac{1}{\rho}\frac{D\boldsymbol{B}}{Dt} - \frac{\boldsymbol{B}}{\rho^2}\frac{D\rho}{Dt} = \frac{1}{\rho}(\boldsymbol{B}\cdot\boldsymbol{\nabla})\boldsymbol{u} \tag{43}$$

$$\frac{D}{Dt}(\frac{\boldsymbol{A}\cdot\boldsymbol{B}}{\rho}) = \boldsymbol{A}\cdot\frac{D}{Dt}(\frac{\boldsymbol{B}}{\rho}) + (\frac{D\boldsymbol{A}}{Dt})\cdot\frac{\boldsymbol{B}}{\rho} \tag{44}$$

$$= \frac{1}{\rho}(A_iB_j\partial_j u_i + B_j u_i\partial_j A_i) - \frac{\boldsymbol{B}}{\rho}.\boldsymbol{\nabla}\Phi = \frac{1}{\rho}B_j\partial_j(A_iu_i) - \frac{\boldsymbol{B}}{\rho}\cdot\boldsymbol{\nabla}\Phi \tag{45}$$

$$\frac{D}{Dt}(\frac{\boldsymbol{A}\cdot\boldsymbol{B}}{\rho}) = (\frac{\boldsymbol{B}}{\rho}\cdot\boldsymbol{\nabla})(\boldsymbol{A}\cdot\boldsymbol{u} - \Phi) \tag{46}$$

Coming back to the magnetic helicity, we can now calculate its variation :

$$\frac{dI_m}{dt} = \int_{V_m}\rho\frac{D}{Dt}(\frac{\boldsymbol{A}\cdot\boldsymbol{B}}{\rho})d\tau = \int_{V_m}(\boldsymbol{B}\cdot\boldsymbol{\nabla})(\boldsymbol{A}\cdot\boldsymbol{u} - \Phi)d\tau \tag{47}$$

As we always have $\boldsymbol{\nabla}.\boldsymbol{B} = 0$ we can also write this expression as:

$$\frac{dI_m}{dt} = \int_{V_m}\boldsymbol{\nabla}\cdot(\boldsymbol{B}(\boldsymbol{A}\cdot\boldsymbol{u} - \Phi))d\tau = \oint_{S_m}(\boldsymbol{B}\cdot\boldsymbol{n})(\boldsymbol{A}\cdot\boldsymbol{u} - \Phi)dS \tag{48}$$

using Gauss theorem to turn the triple integral into a double one.

Now, let's assume that S_m is a material surface, with the interior V_m, on which $\boldsymbol{B}.\boldsymbol{n} = 0$ permanently. We can use Gauss theorem, to change the integral, and we obtain :

$$\frac{dI_m}{dt} = \oint_{S_m} (\boldsymbol{B} \cdot \boldsymbol{n})(\boldsymbol{A} \cdot \boldsymbol{u} - \Phi) dS = 0 \tag{49}$$

If we now no longer neglect the dissipation :

$$\frac{dI_m}{dt} = \lambda \int_{V_m} (\boldsymbol{B} \cdot \boldsymbol{\nabla}^2 \boldsymbol{A} + \boldsymbol{A} \cdot \boldsymbol{\nabla}^2 \boldsymbol{B}) d\tau \tag{50}$$

1.7 Magnetic Buoyancy

The magnetic buoyancy is easy to understand. Where there is a magnetic field, a term appears in the equations, which can be considered as a pressure :

$$P_{mag} = \frac{B^2}{2\mu_0} \tag{51}$$

The material with an internal magnetic field will have the same pressure as the exterior. As a consequence, the thermal pressure of the material will decrease, so that

$$P_{th}^{int} + P_{mag}^{int} = P_{th}^{ext} \tag{52}$$

In order to decrease the thermal pressure, the density will get smaller, which will lead to the phenomena of buoyancy. This buoyancy is a consequence of different density, and the expression of the induced acceleration is :

$$\boldsymbol{a}_{\text{buoy}} = \frac{\delta\rho}{\rho} \boldsymbol{g} \tag{53}$$

In most of the simulations, the gas is ideal, with the polytropic index $\gamma = 5/3$. As a consequence, small variations in density are easily related to small variations in pressure and small variations in entropy,

$$\frac{d\rho}{\rho} = \frac{1}{\gamma} [c_V \frac{dP}{P} - ds] \tag{54}$$

To have a simple model, we can first assume that the variation of pressure is only a consequence of the magnetic field, and we thus ignore the variations of temperature which could induce other density variations.

1.8 Stratification

The aim of this project is to study the influence of the buoyancy on the dynamo. In the simulations, the gas is considered as a perfect one. The adiabatic index is then $\gamma = 5/3$. The initial stratification is polytropic, with an index $m = 1.6$. The gas is stably stratified. This means that the entropy increases with z (upwards). In the Pencil Code, this is implemented with following equations :

$$\frac{s}{c_P} = -\gamma \frac{z - z_{\text{infty}}}{c_{s0}^2} \tag{55}$$

$$ln(\frac{\rho}{\rho_0}) = -\gamma \frac{z - z_{\text{infty}}}{c_{s0}^2} \tag{56}$$

However, this was one big problem we tackled in the simulations. In fact, we absolutely wanted to avoid convection appearing, because then there would be vertical motions which were not due to magnetic buoyancy. It would then be impossible to make the difference between what is due to the magnetic buoyancy, and what is due to convection. Convection could appear if the gas is no longer stably stratified, it means if the entropy, instead of increasing, decreases with height. This situation appeared if there was too much heating and not enough cooling. Then, the gas would be heated, and the entropy increased, but with some boundary conditions on the top surface, it could lead to a reverse of the entropy slope.

As long as the slope of entropy stayed positive, the gas would be stably stratified. Of course, the entropy changes in a very meaningful way during the simulation, due to the heating and to the shear. As a consequence, we had to check regularly this slope.

For instance in the upper picture, we can see that the entropy and the entropy slope are both increasing. It means that the gas is still stably stratified at every height. What is not very intuitive, and is revealed by the picture, is that by heating the gas, and under those particular boundary conditions, the gas becomes stabler with time.

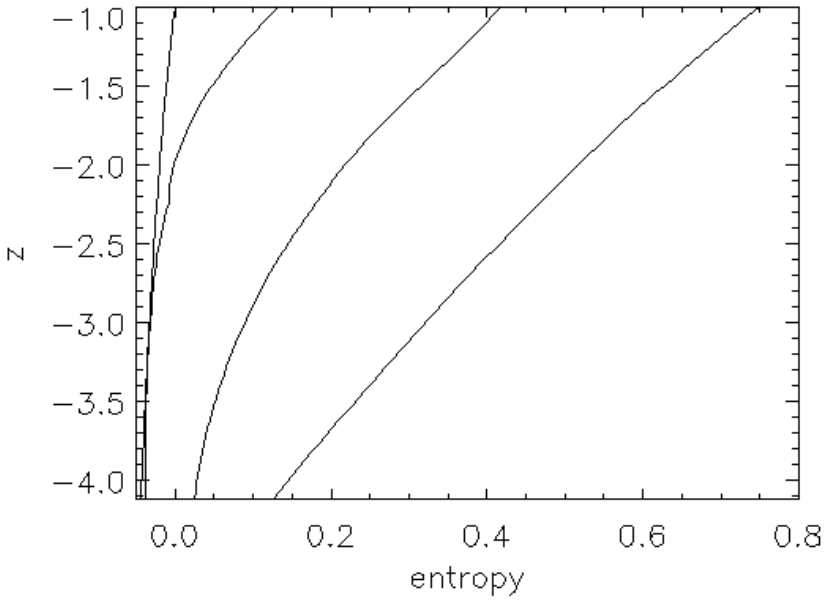

Figure 1: evolution of the entropy, at t=0, t=8, t=85 and t=8440

2 Energy considerations

In order to better understand the magneto, it is useful to adopt an energetic point of view. There are four different kinds of energy, which can be transferred from one into another form : magnetic energy, kinetic energy, potential energy, and thermal energy, which are defined as follows :

$$E_{mag} = \int \frac{B^2}{2\mu_0} dV \tag{57}$$

$$E_{kin} = \frac{1}{2} \int \rho v^2 dV \tag{58}$$

$$E_{th} = \int \rho e dV \tag{59}$$

$$E_{pot} = \int \rho g z dV \tag{60}$$

In our simulations, there are just two inputs or outputs of energy : energy given by the shear, which can allow a dynamo to grow, and radiative energy gained or lost at the top and the bottom of the studied

box. These energies are defined as follows :

$$\epsilon^{\mathrm{s}}_{\mathrm{Kin}} = \int S\rho u_x u_y dS \qquad \epsilon^{\mathrm{s}}_{\mathrm{Mag}} = -\int S B_x B_y dS \tag{61}$$

$$F^{\mathrm{rad}}_{\mathrm{bot}} = \int_{\text{bottom face}} -K\boldsymbol{\nabla} T dS \qquad F^{\mathrm{rad}}_{\mathrm{top}} = \int_{\text{top face}} -K\boldsymbol{\nabla} T dS \tag{62}$$

The energy can be exchanged between these different types as is explained in following graph

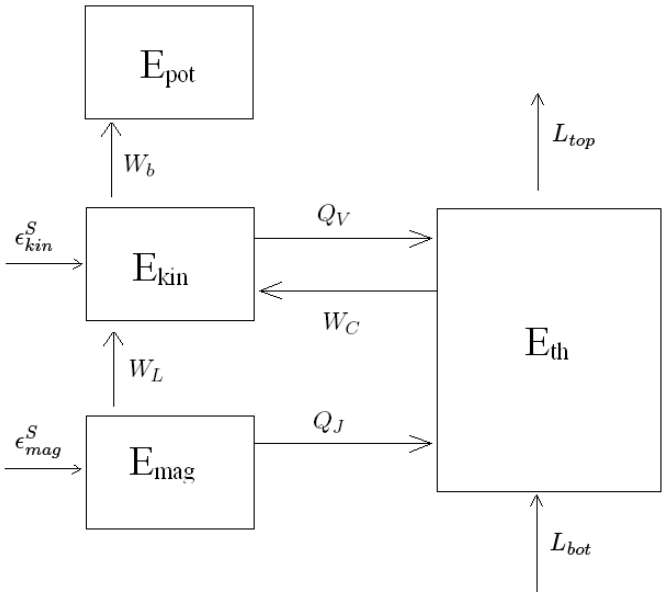

Figure 2: Transfers of energy

The various works have such expression :

$$W_{\mathrm{Lor}} = \int \boldsymbol{u}.(\boldsymbol{j} \times \boldsymbol{B}) dV \tag{63}$$

$$W_{\mathrm{buoy}} = \int \rho u_z g dV \tag{64}$$

$$W_{\mathrm{comp}} = \int -P\boldsymbol{\nabla}.\boldsymbol{u} dV \tag{65}$$

$$\epsilon_{\rm K} = 2 \int \nu\rho \overset{\leftrightarrow 2}{S} \, dV \tag{66}$$

$$\epsilon_{\rm M} = \int \eta\mu_0 \boldsymbol{J}^2 dV \tag{67}$$

In all these terms, one can notice the energy coming from Lorentz force, which couples kinetic and magnetic energy.

$$P_{\rm L} = < \boldsymbol{u}\cdot(\boldsymbol{J}\times\boldsymbol{B}) > = \frac{1}{\mu_0} < \boldsymbol{u}\cdot[(\boldsymbol{\nabla}\times\boldsymbol{B})\times\boldsymbol{B}] > = \frac{1}{\mu_0} < \boldsymbol{u}\cdot(\boldsymbol{B}\cdot\boldsymbol{\nabla}\boldsymbol{B}) - \boldsymbol{u}\cdot\boldsymbol{\nabla}(\frac{B^2}{2}) > \tag{68}$$

with

$$< \boldsymbol{u}\cdot\boldsymbol{\nabla}(\frac{B^2}{2}) > = -\frac{1}{2} < B^2 \ \cdot \boldsymbol{u} >$$

3 Parameters of the simulations

3.1 The Pencil Code

The simulations were made with the Pencil Code. It is a public code used in magnetohydrodynamics, which uses sixth-order explicit finite differences in space and third order accurate time stepping model.

3.2 Initial conditions

Initially, the flux does not move, and is not sheared. There is a magnetic field present, in the form of a flux tube. The expression of this magnetic field is :

$$B_x = 2\frac{1+\epsilon\ \cos(kx)}{1+r^2/R_0^2} \tag{69}$$

$$B_y = \frac{y\ \epsilon\ k\ \sin(kx)}{1+r^2/R_0^2} \tag{70}$$

$$B_z = \frac{(z-z_0)\ \epsilon\ k\ \sin(kx)}{1+r^2/R_0^2} \tag{71}$$

In all the simulations, we chose $\epsilon = 0.3$, $k = \frac{2\pi}{L_x} = \frac{\pi}{2}$, $R_0 = 0.2$.

3.3 Boundary conditions

Before running a simulation, numerous choices were possible concerning the boundary conditions. First of all, and in a natural way, it was chosen to work in a closed box, which meant that at the top and at the bottom of the box, $\boldsymbol{u}$ has a zero-value in the z-direction. As a consequence, a symmetric condition was for u_x and u_y, and an antisymmetric one for u_z.

Concerning the density, the derivative was chosen to be antisymmetric, which means that the density had to be constant at the border.

The magnetic field had to have the same boundary conditions than the velocity field. We also choose a symmetric condition for B_x and B_y, and an antisymmetric one for B_z.

The biggest problem was about the entropy, and its boundary conditions. We could choose between 'a', 'a2', 'c1', 'cT' as boundary conditions. The first one, 'a', meant that the entropy had to be zero at the top and at the bottom of the box. The second one imposed the first derivative to be zero. 'c1' imposed the heating and cooling flux

to be constant, equal to their initial value. And finally 'cT' fixed the temperature on the top and the bottom faces. It was difficult to find out which condition was the best one. In fact, the major problem of these simulations was to avoid convection.

3.4 Other parameters

In all the simulations, we had to fix some physical values, as the viscosity, the magnetic diffusivity, and the heat conductivity. It was hard to give any sense to these parameters, because as they were non dimensional, I could not turn them into the real values. Moreover, the simulations cannot reproduce exactly the behaviour of the sun, because we have too little meshpoints. As a consequence, the spectrum of energy is not good enough, and we already know that we cannot have access to any phenomenon. The simulation should not reproduce the sun, but allows us to understand some physics, which could then be applied to the sun.

4 Simulations

4.1 Summary of the simulations

run	Boundary conditions	K	ν	η	m	collapse
64b	c1:cT	5.10^{-2}	5.10^{-2}	5.10^{-2}	1.6	?
64d	c1:cT	5.10^{-3}	5.10^{-3}	5.10^{-4}	1.6	?
64e	c1:cT	5.10^{-3}	5.10^{-3}	1.10^{-4}	1.6	?
64f	c1:cT	1.10^{-3}	5.10^{-3}	1.10^{-4}	1.6	?
64viob	c1:cT	0.1	2.10^{-3}	5.10^{-4}	2	yes
ad64a	a	2.10^{-3}	2.10^{-3}	5.10^{-4}	1.5	?
ad64b	a	2.10^{-3}	2.10^{-3}	1.10^{-4}	1.5	?
c1_64a	c1	2.10^{-3}	2.10^{-3}	5.10^{-4}	1.5	?
c1_64a2	c1	2.10^{-3}	2.10^{-3}	5.10^{-4}	1.5	?
c1_64b	c1	2.10^{-3}	2.10^{-3}	1.10^{-4}	1.5	?
c1_64c	c1	0.1	2.10^{-3}	5.10^{-4}	1.6	?
c1_64d	c1	0.1	2.10^{-3}	5.10^{-4}	1.6	no
c1cT_64a2	c1:cT	0.1	2.10^{-3}	5.10^{-4}	3	?
c1cT_64a3	c1:cT	0.1	2.10^{-3}	5.10^{-4}	3	?
c1cT_64b	c1:cT	0.1	2.10^{-3}	5.10^{-4}	1.5	?
c1cT_64d	c1:cT	0.1	2.10^{-3}	5.10^{-4}	1.5	?
c1cTnu_64	c1:cT	0.1	1.10^{-2}	5.10^{-4}	1.5	?
ce_64a	ce	1.10^{-3}	2.10^{-3}	2.10^{-5}	1.6	?
ce_64o	ce	1.10^{-3}	5.10^{-3}	1.10^{-4}	1.6	?
c1cT_64e	c1:cT	0.1	1.10^{-2}	5.10^{-4}	1.6	?
c1cT_64g	c1:cT	0.1	2.10^{-3}	5.10^{-4}	1.6	no
a_64a	a2	0.1	2.10^{-3}	5.10^{-4}	1.6	no
a_64b	a2	1.10^{-3}	2.10^{-3}	5.10^{-4}	1.6	?
ac1_64a	a2:c1	0.1	2.10^{-3}	5.10^{-4}	1.6	no
acT_64a	a2:cT	0.1	2.10^{-3}	5.10^{-4}	1.6	yes

4.2 Situation without shear

As said above, there is initially a horizontal magnetic tube, centered around $z_0 = -3$, i.e. in the lower quarter of the box. If there was no shear, then the gas pressure would decrease where there is a strong magnetic field. As a consequence, the density would also decrease, and the buoyancy work would make the gas ascend. We can see that it is happening thanks to following picture, which represents the mean magnetic field averaged in the x and y directions, respectively.

We can first see that the magnetic field in the x direction ascends

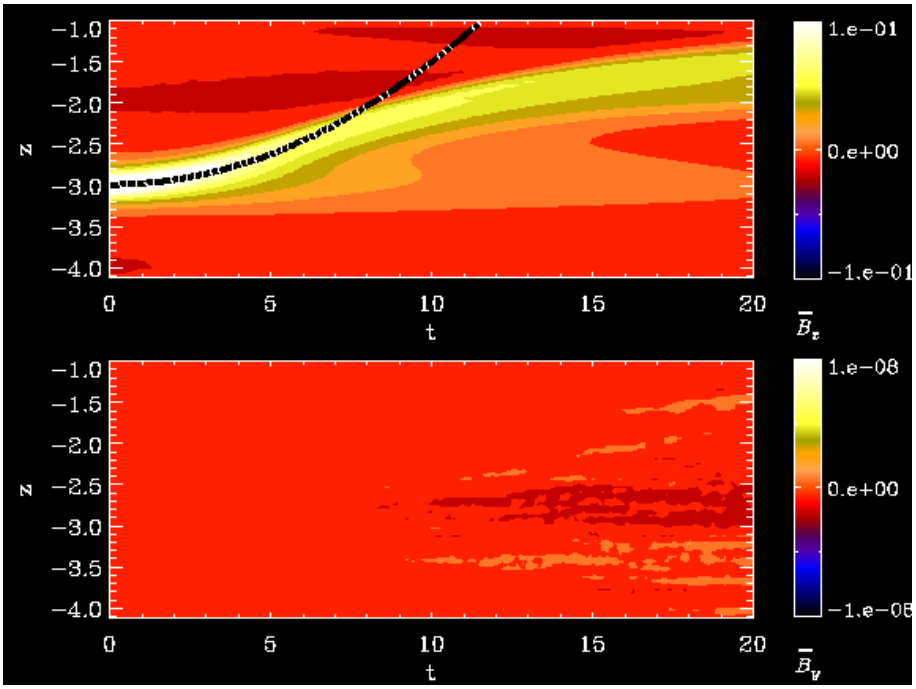

Figure 3: Evolution of the magnetic field without shear

at early times. This reveals the ascension of the gas where there is this magnetic field. In fact, with the approximation of a frozen fluid, we know that the magnetic field is twisted by the velocity field so that it has the same shape. We can also see that the upwards motion can be well fitted for low times, ($t < 8$) by a parabola of expression: $0.015 * t^2 - 3$. This means that the buoyancy force is constant at the beginning.

Another conclusion of this first picture is that there is no conversion of B_x into B_y, or so little conversion that it can be ignored.

We can also look at the picture of the velocity, when there is no shear. We can then see that there is almost no motion in the x and y directions. But as foreseen, there is a lot of motion in the z-direction. We can see two sound waves propagating in the box. As there are boundary conditions, these waves can keep propagating. The waves come from the difference of pressure. The first one goes upwards, while the second one goes downwards. After a short time, these two waves seem to mix, and we can just see an oscillation in the z-direction.

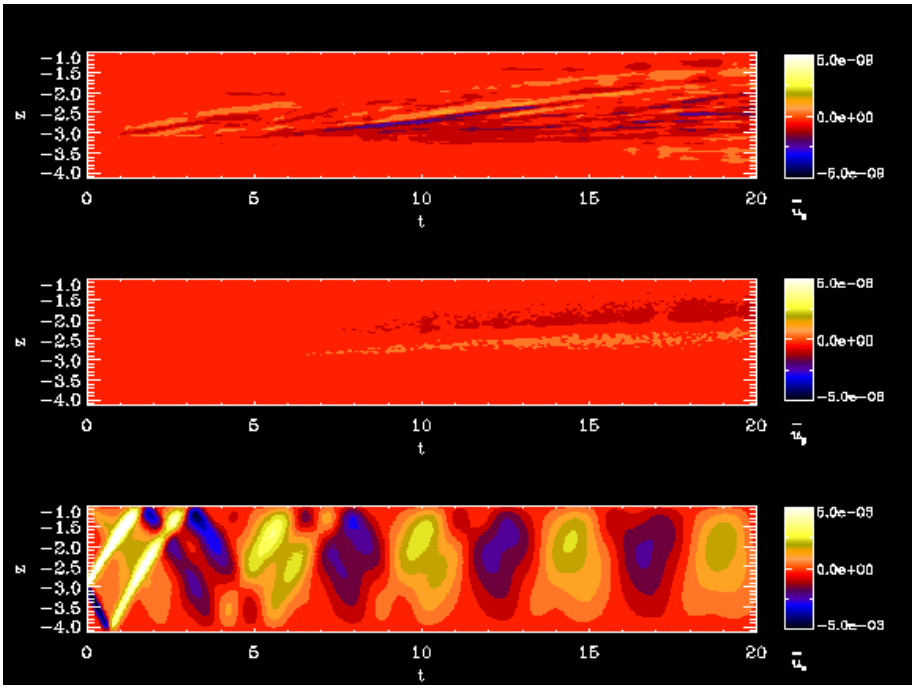

Figure 4: Evolution of the kinetic field without shear

4.3 Initial evolution of the magnetic and kinetic fields

By putting shear in the simulation, we are now changing many things. First, we create the ω-effect. As seen in the theory, it will create a strong magnetic field in the y-direction from the field in the x-direction. Then, it will also give energy to the system, into kinetic energy, but also into magnetic energy.

All the following simulations have the same parameters, but different boundary conditions. It seems that the short-term consequences of the boundary conditions are very weak, so I will just speak of one case.

We notice immediately that there is a very big difference in the y direction. There is a strong magnetic field created. In a very short time ($t \approx 10$), it happens to be as strong as B_x. This fits well the theoretical calculations which were done in the theoretical presentation. In fact, we had

$$\frac{\partial B_y}{\partial t} \approx S B_x$$

This expression implies that, if B_x is considered as constant, B_y becomes as strong as B_x in a time $\tau_{\text{Shear}} = 1/|S| = 10$, which is what

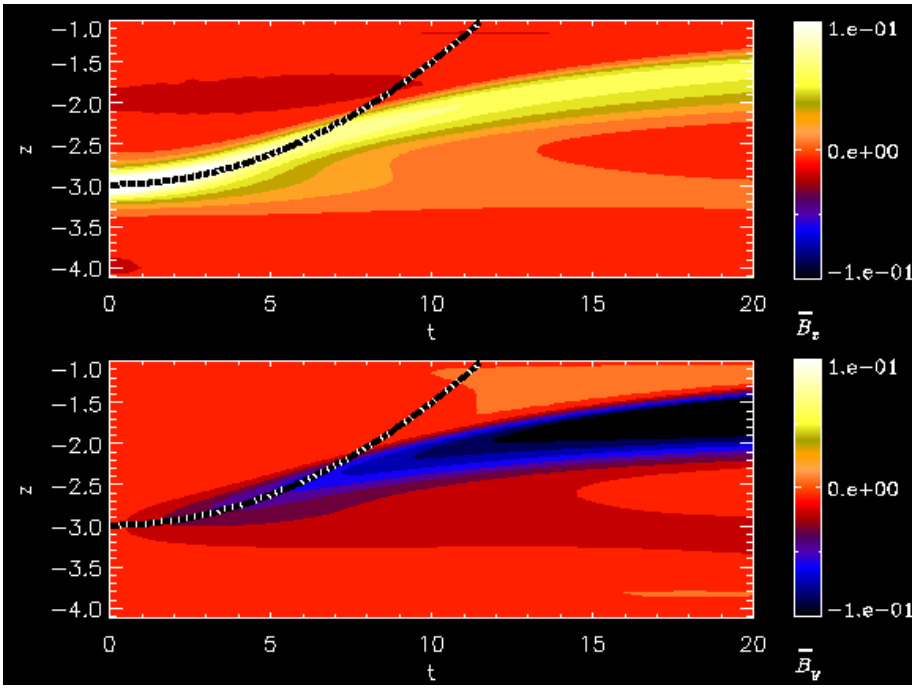

Figure 5: Evolution of the magnetic field with shear

we can see in the picture.

We can also notice that the shear does not really change the component of the B_x-field: there is still the same curve which fits the ascension of the field at the shorter times. However, we can still notice that, while there was a slight decay without shear, this does not happen anymore in the presence of shear. This is surprising and suggests the presence of some additional amplification mechanism.

There is no big difference between the kinetic evolution with or without shear. We still can see the sound waves propagating upwards and downwards in the z-velocity field. As there is the same scale in the x and y component, we can easily compare them. We can notice that when there is shear, the velocity field increases at the top of the box, which was not the case without shear.

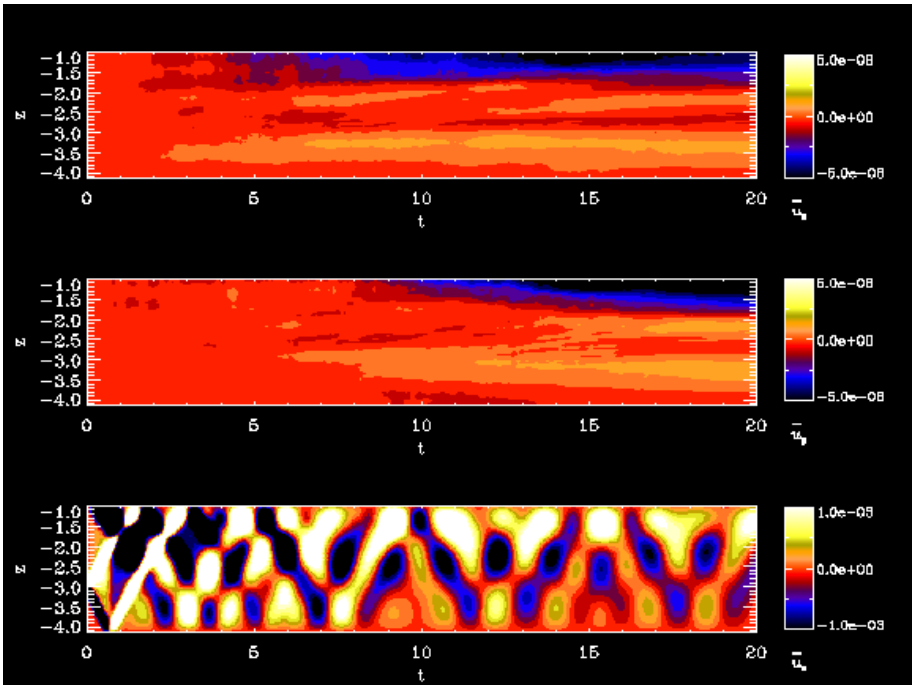

Figure 6: Evolution of the kinetic field with shear

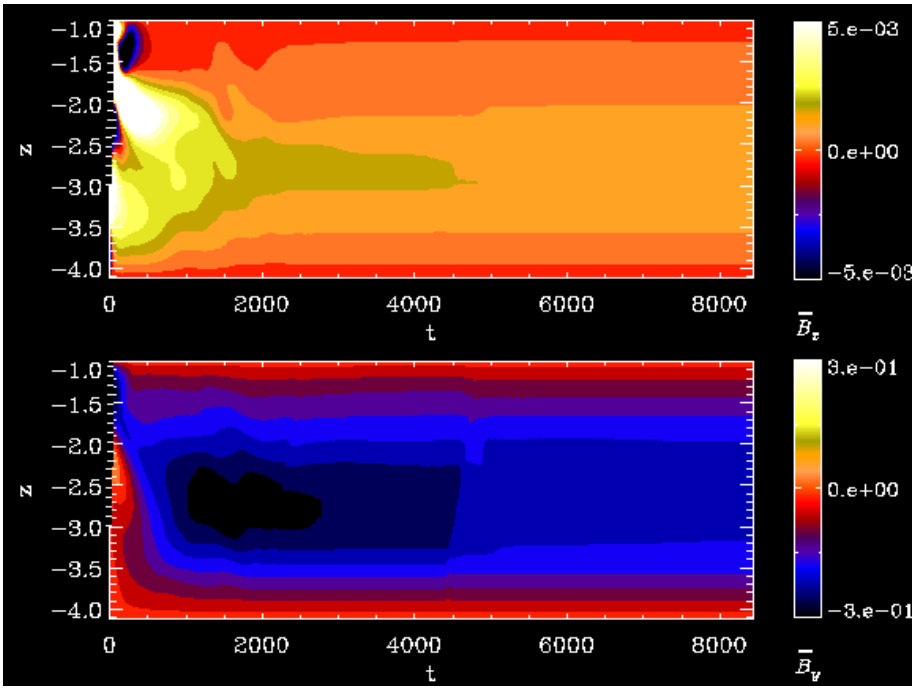

Figure 7: Evolution of the magnetic field with shear

4.4 Long-term evolution of the kinetic and magnetic fields

In this subsection, I will focus on the simulation with an $'a2'$ boundary condition at the top and the bottom. It is noticeable that even if the boundary conditions can modify deeply the results, there is always the same global behaviour, which is not yet understood.

We can here notice that there is a global decay of the magnetic field with time. However, given that the resistive time scale is less than 1000 time units, and as the simulation ran for more than 8000 time units, we can at least call it a long-lived turbulence. But other simulations which ran during more than 16000 time units showed that the behaviour seems steady after such a long time, so it is probable that this system really is a dynamo.

We notice that B_x decays a lot at the beginning, and then stays steady at a value which is about one percent of its initial value, and of course much less localized. It is however relevant to notice that this x-component of the magnetic field seems still to be around $z = -3$, which was its initial location, even if after a very short time it had ascended far away from this position.

The y-component increases significantly at the beginning, then decays slowly during two or three magnetic-dissipation-times, and then stays steady. After 5000 time units, the graphs really show us that everything is steady. This y-component is also centered around $z = -3$.

This spatial distribution of the magnetic field, which is much stronger in the middle of the box than up or down, can lead to turbulence driven by magnetic buoyancy. We can indeed see that at the top of the box, there are motions of convection, but which are probably due to magnetic buoyancy, given that the entropy slope is still positive.

It is also interesting to look at the velocity profile. This profile seems to be divided into three different parts. First, from the beginning and until around 1000 time units, there is a strong vertical velocity, and almost no horizontal velocity. Then, between 1000 and 5000 time units, we can see a horizontal velocity developing at the top of the box, while there are still rapid vertical motions. After 5000 time units, the velocity field also seems to be steady. It may also be relevant to notice the reversal of sign in the y-velocity.

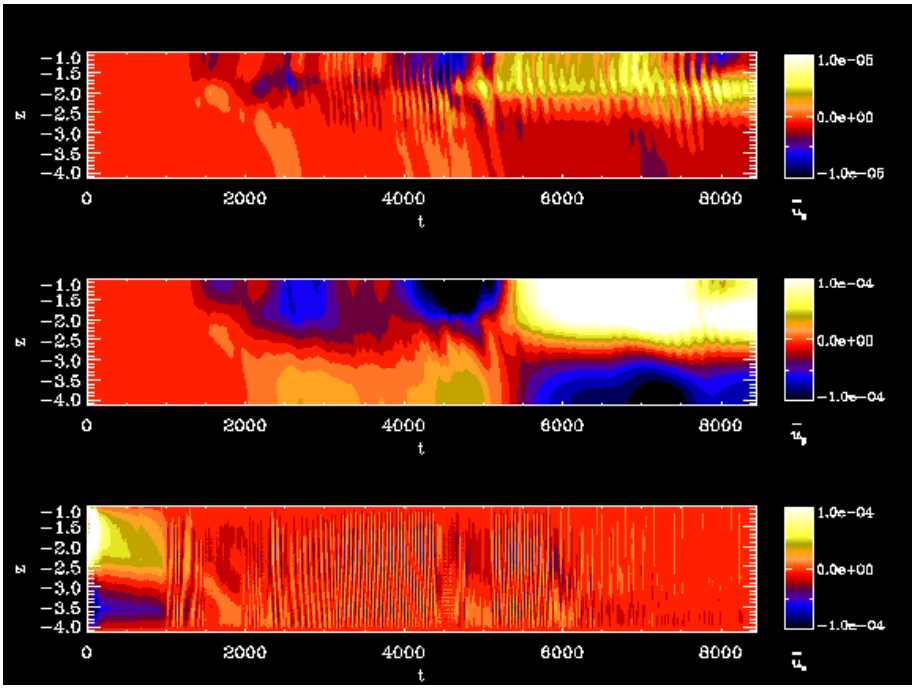

Figure 8: Evolution of the kinetic field with shear

4.5 Influence of boundary conditions

In the following simulations, all the parameters were the same except the z-boundary conditions for the entropy. Given the differences, it seems to be a crucial choice. Of course, no boundary condition will be perfect, but we would like to find one which would allow an increase of the magnetic field due to turbulence driven by magnetic buoyancy.

These simulations were run under with the following parameters : $K = 0.1$, $\nu = 2.10^{-3}$ and $\eta = 5.10^{-4}$. The polytropic index was 1.6, and the stratification as described above, the same as the stratification in the article of Brummell, Cline and Cattaneo was.

Each simulation gives different results from the other ones. We can draw that in following table.

bcz	$< u^2 >$	$< b^2 >$	x-symmetry	entropy slope	shear energy ratio
a2:a2	2.10^{-5}	0.0225	u_z, B_x, B_y B_z antisymmetric	0.20	25
a2:c1	6.10^{-6}	0.029	u_z, B_x,B_y,B_z neither symmetric B_z nor antisymmetric	0.20	40
c1:c1	3.10^{-4}	0.0037	B_x,B_y,B_z neither symmetric B_z nor antisymmetric	0.013	0.13

4.6 Other observations

4.6.1 Initial condition

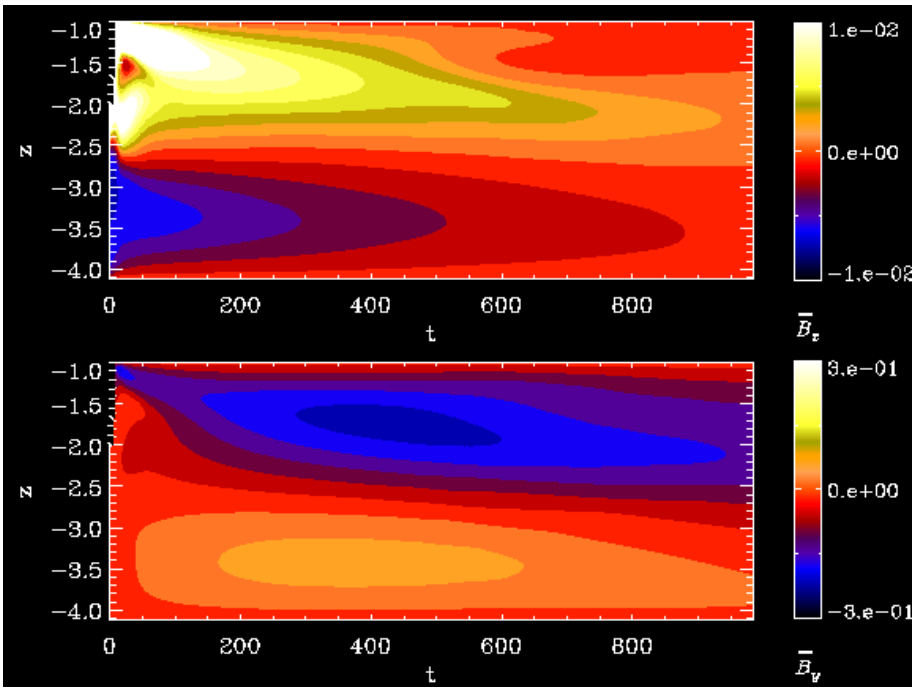

Figure 9: Evolution of the magnetic field

We would like to have a system which does not depend too much on the initial conditions. This would mean that whatever we write there, it could still be a valid model to apply for the Sun, or other stars. However, by localizing the initial magnetic tube at another height, it seems that we have different results. In this simulation, with $z_0 = -2$, the initial magnetic tube was localized in the top half of the box. The first evolution is identical to the one described above. However, when we look at the evolution at later time (even if they are smaller than the magnetic dissipation time), we can clearly notice that the magnetic fields are no longer centered around $z \approx -3$, as it was the case in

the first simulation. Now, B_y has two different signs, a negative one, which is also the stronger component, centered around $z = -2$. The x-component is still decaying, but now there are also two different signs. In this situation, there are two maxima of magnetic energy, one at $z \approx -3.5$ and one at $z \approx -2$. It may also be due to the fact that the simulation did not run long enough.

4.6.2 Influence of the heat conductivity

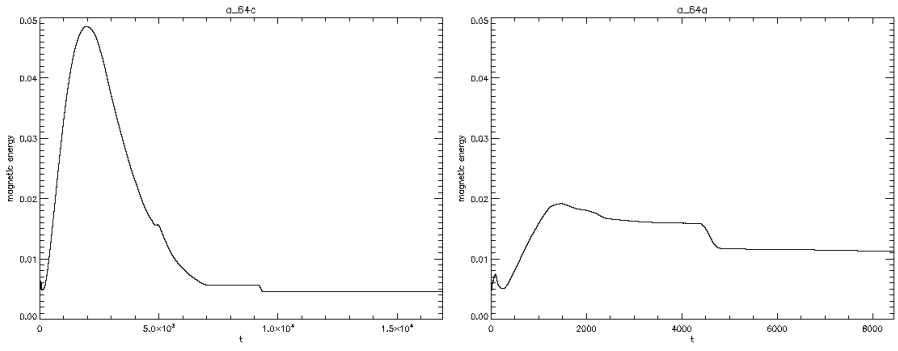

Figure 10: Variation of magnetic energy for $K = 0.01$ and for $K = 0.1$

We can here easily find the influence of the heat conductivity on the dynamo process. First, we should notice that, if the energy scale is the same for both graphs, the time scale is different. So we should be careful about that.

However, we can easily see that a large heat conductivity does not allow the magnetic energy to grow quickly. In fact, it seems that the first graph has been truncated, compared to the other graph and this for times shorter than 4500 time units. This may show that there is not just magnetic buoyancy working in such a simulation, but also thermal buoyancy. The magnetic energy is indeed converted into thermal energy thanks to dissipation, and with a bigger heat conductivity, this heat will get diffuse sooner, which explains why there is no real temperature gradient, and as a consequence there is no significant thermal buoyancy for $K = 0.1$. On the other hand, with a smaller K, there can be a larger temperature gradient, which creates thermal buoyancy, and makes the magnetic field stronger.

Another important observation is that after a certain time, the simulation with weaker heat conductivity has a weaker magnetic field than the other one. It is not yet well understood why it is like that.

Conclusion

We can draw here the following conclusion. It seems that there can be a dynamo process due to the presence of shear. This shear converts an initial poloidal magnetic field into a stronger toroidal magnetic field through the ω-effect. This allows then magnetic buoyancy to work, and from the turbulence created by the magnetic buoyancy, the α-effect can create again a toroidal magnetic field.

However, it is not yet understood why the magnetic energy seems to be steady after a longer time. Simulations should also run for longer time so that we can be sure that there is a real dynamo, and not just long-lived turbulence.

If this is really true, it may have significant consequences for the solar dynamo, as the tachocline presents an important shear.

Personally, this internship made me discover the world of research and I am glad to have done it. However, I needed too many weeks to understand how the simulations worked and how to work with their results, but at the end of the internship, I think I had become more efficient.

References

[1] H.K. Moffatt *Magnetic field generation in electrically conducting fluids*

[2] K S.Cline, N H. Brummell, F Cattaneo *Dynamo action driven by shear and magnetic buoyancy*

[3] A. Brandenburg, K.-H. Rädler, M. Rheinhardt, P.J. Käpylä *Magnetic diffusivity tensor and dynamo effects in rotating and shearing turbulence*